

1 **Title page**

2 Names of the authors: Katja Magdić Košiček<sup>1</sup>, Ljudmila Benedik<sup>2</sup>, Marijan Nečemer<sup>2</sup>, Branko  
3 Vodenik<sup>2</sup>, Benjamin Zorko<sup>2</sup>, Željko Grahek<sup>1</sup>, Ivana Tucaković<sup>1\*</sup>

4  
5 Title: **Gamma spectrometry coupled with electrodeposition for <sup>55</sup>Fe determination in solid**  
6 **samples containing significant amount of total iron**

7  
8 Affiliation(s) and address(es) of the author(s):

9 <sup>1</sup> Ruđer Bošković Institute, Bijenička cesta 54, 10 000 Zagreb, Croatia

10 <sup>2</sup> Jožef Stefan Institute, Jamova 39, SI-1000 Ljubljana, Slovenia

11 E-mail address of the corresponding author: [ivana.tucakovic@irb.hr](mailto:ivana.tucakovic@irb.hr)

12  
13  
14 **Author contributions statement**

15 All authors contributed to this article. Conceptualization: Katja Magdić Košiček, Ivana  
16 Tucaković, Benjamin Zorko; Methodology: Ljudmila Benedik, Marijan Nečemer, Katja Magdić  
17 Košiček, Ivana Tucaković; Formal analysis and investigation: Benjamin Zorko, Marijan  
18 Nečemer, Branko Vodenik, Ljudmila Benedik, Ivana Tucaković; Writing - original draft  
19 preparation: Katja Magdić Košiček, Ivana Tucaković; Writing - review and editing: Ljudmila  
20 Benedik, Benjamin Zorko, Marijan Nečemer, Branko Vodenik, Željko Grahek; Supervision:  
21 Željko Grahek, Benjamin Zorko;

22 **Gamma spectrometry coupled with electrodeposition for  $^{55}\text{Fe}$  determination**  
23 **in solid samples containing significant amount of total iron**

24

25 Katja Magdić Košiček<sup>1</sup>, Ljudmila Benedik<sup>2</sup>, Marijan Nečemer<sup>2</sup>, Branko Vodenik<sup>2</sup>, Benjamin  
26 Zorko<sup>2</sup>, Željko Grahek<sup>1</sup>, Ivana Tucaković<sup>1\*</sup>

27 <sup>1</sup> *Ruđer Bošković Institute, Bijenička cesta 54, 10 000 Zagreb, Croatia*

28 <sup>2</sup> *Jožef Stefan Institute, Jamova 39, SI-1000 Ljubljana, Slovenia*

29

30 **Abstract**

31 This study demonstrates the potential of gamma spectrometry coupled with electrodeposition as  
32 a sample preparation technique for determination of  $^{55}\text{Fe}$  in complex solid samples with high  
33 iron content. Electrodeposition has proven to be a reliable method for obtaining thin,  
34 homogeneous films containing up to 50 mg of total iron. In contrast, ammonium  
35 pyrrolidinedithiocarbamate precipitation method shows inhomogeneity and significant film  
36 thickness at 0.5 mg of iron. The efficiency correction function for gamma-spectrometric  
37 measurements based on the total iron content was introduced.

38

39

40 **Keywords**

41  $^{55}\text{Fe}$ ,  $\gamma$ -ray spectrometry, electrodeposition, APDC precipitation, solid samples, radioactive  
42 waste

43

## 44            **Introduction**

45            Nuclear power plants contribute to 10 % of global electricity production, emphasising  
46 their significant role in the energy sector [1]. However, around 70 % of nuclear reactors have  
47 been in operation for more than 30 years and according to International Atomic Energy Agency  
48 (IAEA), around 200 reactors will have to be decommissioned in the next 20 years [2].  
49 Decommissioning generates significant amounts of radioactive waste that must be thoroughly  
50 characterized and managed [3].

51            Radiological characterization is essential in order to precisely identify and quantify the  
52 radionuclides present in the waste. This includes measuring the content of various radionuclides  
53 in materials such as radioactive waste, construction materials, soil, sediments, water and plants.  
54 The results obtained are crucial for estimating the total radioactivity imposed into the  
55 environment. The radioactivity in these materials comes mainly from activation and fission  
56 products, including isotopes like  $^3\text{H}$ ,  $^{14}\text{C}$ ,  $^{36}\text{Cl}$ ,  $^{41}\text{Ca}$ ,  $^{60}\text{Co}$ ,  $^{55}\text{Fe}$ ,  $^{63}\text{Ni}$ ,  $^{90}\text{Sr}$ ,  $^{129}\text{I}$ ,  $^{133}\text{Ba}$ ,  
57  $^{137}\text{Cs}$ ,  $^{152}\text{Eu}$ ,  $^{154}\text{Eu}$  and certain transuranics [4].

58            Among these radionuclides,  $^{55}\text{Fe}$  is of particular importance due to its effects on the  
59 environment and health. When ingested (either by inhalation, ingestion or skin contact), as much  
60 as 80 % of  $^{55}\text{Fe}$  is absorbed by the liver and 1.3 % by the spleen. The remainder is distributed to  
61 other organs and tissues and has a dangerous effect on human health [5]. In steels,  $^{55}\text{Fe}$  together  
62 with  $^{60}\text{Co}$  is the predominant radionuclide in the first 10 to 20 years after the shutdown of a  
63 nuclear reactor.  $^{55}\text{Fe}$  (half-life,  $t_{1/2} = 2.7$  years) is produced in nuclear power plants by neutron  
64  $(n, \gamma)$  activation of  $^{54}\text{Fe}$  and  $(n, 2n)$  activation of  $^{56}\text{Fe}$ , and emits X-rays (5.9 keV) during the  
65 decay by electron capture (EC). From an analytical point of view,  $^{55}\text{Fe}$  is a difficult to measure  
66 (DTM) radionuclide that cannot be characterized by direct measurements. The analytical

67 procedure for  $^{55}\text{Fe}$  determination usually involves several steps, including decomposition of the  
68 real sample material, separation of the iron from the matrix elements and other radionuclides and  
69 final preparation of the  $^{55}\text{Fe}$  source sample into a form suitable for liquid scintillation counting  
70 (LSC) and/or X-ray spectrometry. Both LSC and gamma ray spectrometry have been used for  
71 measurements of  $^{55}\text{Fe}$  and compared in the literature [6 - 12].

72 LSC offers high sensitivity, enabling accurate measurements even at low iron  
73 concentrations, efficient detection of  $^{55}\text{Fe}$  without complex sample preparation, determination of  
74  $^{55}\text{Fe}$  from different sample types, etc. However, when analyzing samples with high total iron  
75 content, such as decommissioning materials, LSC encounters significant challenges. The  
76 presence of large amounts of iron leads to colour quenching that reduce detection efficiency.  
77 Another challenge in the determination of  $^{55}\text{Fe}$  with LSC is the background radiation. The low  
78 energy emission of  $^{55}\text{Fe}$  can overlap with background radiation and other low energy events in  
79 the scintillation cocktail, making it difficult to distinguish  $^{55}\text{Fe}$  counts from background noise.

80 Gamma ray spectrometry offers a possible solution to these problems. It is also a widely used  
81 technique, as laboratories specialized in the measurements and monitoring of environmental  
82 radioactivity in different types of samples are regularly equipped with gamma-ray spectrometers.  
83 The golden standard for gamma-spectrometry today are high purity germanium detectors (HPGe)  
84 with high resolution. Although  $^{55}\text{Fe}$  has low emission energy of 5.9 keV, which makes it difficult  
85 to detect by gamma spectrometry, the use of an HPGe detector with thin windows that allow the  
86 detection of photons across a wide energy range (3 keV – 3 MeV) can solve this problem.  
87 However, despite this improvement, reports on the determination of  $^{55}\text{Fe}$  in real samples by  
88 gamma ray spectrometry are still scarce. This is mainly due to the problem of attenuation, which  
89 requires the sample to be in the form of a thin and homogeneous film, making sample

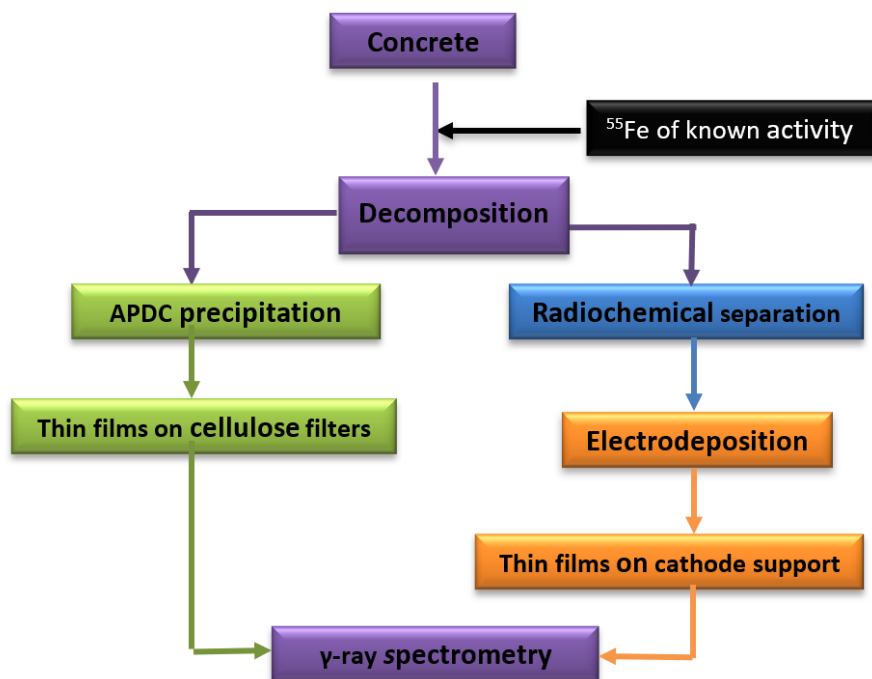
90 preparation a critical but challenging task. The high attenuation of low-energy photons in the  
91 material is a key problem for this type of measurement, as the detection efficiency is highly  
92 dependent on the thickness of the prepared sample. In addition, the low energy region of the  
93 spectrum can be populated by interfering lines from other radionuclides present and by the  
94 Compton background. Consequently, the formation of very thin, homogeneous iron films  
95 isolated from the sample material is essential for obtaining accurate and reproducible results. The  
96 electrodeposition (ED) method is advantageous for this purpose, especially when low detection  
97 limits are required. Although there are numerous studies on the electrodeposition of iron [13 –  
98 20], researches focused on preparation of thin, homogeneous  $^{55}\text{Fe}$  films for gamma-ray  
99 spectrometry analysis are quite limited [21 - 24]. The main objective of this study is therefore to  
100 develop and optimise the electrodeposition method for preparation of thin iron films as solid iron  
101 sources for gamma ray spectrometric measurement of low  $^{55}\text{Fe}$  activities in solid samples, such  
102 as concrete and other radioactive waste materials, using high purity germanium detectors. In  
103 addition to ED, iron is also precipitated using ammonium pyrrolidinedithiocarbamate (APDC).  
104 Dithiocarbamates are known to selectively and strongly bind various metal ions and form stable  
105 metal complexes [25 - 27] which favors their application in many different fields [28]. In this  
106 study the APDC precipitation method on cellulose filters which results in thin and homogeneous  
107 iron complex films [29,30] was performed and compared with electrodeposition.

108

## 109 **Materials and methods**

110 Four stages of analytical procedure used for the preparation of thin solid film  $^{55}\text{Fe}$  source  
111 samples from real concrete samples are schematically shown in the Fig. 1:

112



113

114 **Fig. 1** Schematic representation of the experimental procedure for the preparation of thin  
115 films for gamma ray spectrometry for the determination of <sup>55</sup>Fe in concrete

### 116 **Sample (concrete) preparation and decomposition**

117 Prior to electrodeposition, the concrete was dissolved by fusion with lithium metaborates.  
118 In this procedure, a known activity of the <sup>55</sup>Fe standard solution ( $A = 812 \text{ Bq/g}$ ) was added to a  
119 weighed amount of pulverized concrete (0.2 to 1 g). The fusion process was carried out in a  
120 Claisse LeNeo furnace at 1050 °C for 23 minutes. Immediately after fusion, the melted sample  
121 was poured into stirred Milli-Q water in a Teflon beaker. The detailed procedure for dissolution  
122 by fusion is described in Trdin and Benedik (2017) [31].

123 Once the sample was completely dissolved, 1 ml of 0.2 M polyethylene glycol was added  
124 dropwise to the solution to form silicates. The beaker was then covered and left overnight to

125 allow the silicates precipitate to form and settle. The resulting solution was centrifuged, filtered  
126 through a Sartorius cellulose nitrate filter (radius of 46 mm and pore size of 0.45  $\mu\text{m}$ ), and then  
127 subjected to further analysis steps.

128

### 129 **Radiochemical separation - separation of iron on TRU resin by HCl elution**

130 In order to prepare concrete samples for electrodeposition, the iron had to be separated  
131 from other interfering elements in the sample. TRU resin (2 g) was used for this purpose as it has  
132 a high capacity for iron and the separation process is simple and fast. The concrete sample,  
133 which already contained the added  $^{55}\text{Fe}$  standard solution, was diluted and evaporated before the  
134 addition of 20 ml of 6 M HCl.

135 This prepared sample was then passed through a column containing TRU resin (preconditioned  
136 with 20 ml of 6 M HCl) at a flow rate of 1 ml/min. The iron was strongly adsorbed onto the  
137 resin, while other components were washed out with 20 ml of 4 M HCl followed by 10 ml of  
138 2 M HCl. Finally, the iron was eluted with 20 ml distilled water.

139 The sample prepared in this way was ready for electrodeposition. When using the APDC  
140 method, this step was skipped.

141

### 142 **Preparation of thin and homogeneous films**

143 Two different methods were used: APDC precipitation and electrodeposition. In both  
144 cases, the aim was to obtain thin, homogeneous, and reproducible films suitable for  $^{55}\text{Fe}$   
145 detection by gamma ray spectrometry.

146

147 APDC precipitation of iron from real concrete samples

148

149 A freshly prepared APDC solution was made by dissolving 0.01 g of APDC in 2 ml of  
150 distilled water and then added to the concrete solution as described in *Sample (concrete)*  
151 *preparation and decomposition* section. The resulting mixture was stirred for 30 minutes and  
152 then filtered through a Sartorius cellulose nitrate filter (radius of 46 mm and pore size of  
153 0.45  $\mu\text{m}$ ) using a Millipore filtration system. Finally, the precipitate deposited on the filter was  
154 dried in air [29].

155 To investigate the correlation between the amount of iron present in the samples and the  
156 accuracy of determining the exact activity of  $^{55}\text{Fe}$  by gamma spectrometry, concrete samples  
157 with different amounts of total iron were used. Also, to additionally validate the results obtained,  
158 the measurements of  $^{55}\text{Fe}$  activity were taken at two different laboratories - Ruđer Bošković  
159 Institute (IRB), Zagreb and at Jožef Stefan Institute (IJS), Ljubljana.

160

161 Electrodeposition of iron

162 The electrodeposition was performed using a custom-built, two-electrode electrochemical  
163 cell made of Teflon. The cell consisted of a hollow Teflon tube with a movable lid to which the  
164 platinum disc anode was attached. The stainless steel (SS) cathode was positioned in a metal jar,  
165 with 3.14  $\text{cm}^2$  of its geometric surface exposed to the electrolyte. The lower part of the Teflon  
166 tube was screwed onto the metal jar, maintaining the same geometry and a distance of 1 cm  
167 between the electrodes.

168 All samples were electrodeposited under conditions written below:

- 169 ○ **Temperature** of  $(25 \pm 2)$  °C; This temperature was chosen because a few experiments  
170 carried out with a cooling system at 15 °C, led to oxalate crystallization and lack of iron  
171 film electrodeposition.
- 172 ○ **Electrolyte:** ammonium oxalate monohydrate (5.7 % w/v, Merck) and 0.5 ml  
173 hydrochloric acid (6 M, Kemika). Ammonium oxalate has been selected for its ability to  
174 form stable complexes with metal ions, including iron ions, which favor the formation of  
175 smooth and uniform deposits. These are of utmost importance in case of  $^{55}\text{Fe}$   
176 determination by gamma-spectrometry, to obtain an iron film that is thin and  
177 homogeneous, to overcome the attenuation problem due to the low energy X-ray  
178 emission of 5.9 keV. The properties of the film should be similar to the properties of  
179 actinides obtained under the same conditions as described in actinide electrodeposition  
180 optimization studies [32 - 35]. Hydrochloric acid, on the other hand, provides a strongly  
181 acidic environment that improves conductivity and facilitates electrodeposition [36, 37].
- 182 ○ **Volume** of the solution: 10 ml, as the electrodeposition of actinides carried out in this cell  
183 has shown that the distances below 5 mm and above 10 mm have a negative influence on  
184 the source preparation. As the same cell with the same electrolyte is used for the iron film  
185 preparation, a similar behavior is to be expected [34].
- 186 ○ **Current** density of  $0.190 \text{ A/cm}^2$  was applied. In view of previous studies [35] in which  
187 current parameters were investigated, several experiments were performed with current  
188 density of  $0.75 \text{ A/cm}^2$ . However, an obvious dissolution of Pt was observed resulting in a  
189 dark film on the cathode surface in about 10 minutes after the start of electrodeposition,  
190 thus preventing further electrodeposition. In view of this fact, further studies were carried  
191 with a current of  $0.190 \text{ A/cm}^2$  [34]. Since the results obtained under these conditions led

192 to high electrodeposition yields in 90 minutes or less (depending on the amount of total  
193 iron present), further studies, including variation of the applied current density, were not  
194 conducted.

#### 195 *Optimization of time of electrodeposition using test solutions*

196 In order to optimize the yield of iron electrodeposition, a series of experiments were  
197 carried out with test solutions. These solutions contained an iron carrier (10 mg to 50 mg) and a  
198 <sup>55</sup>Fe standard solution (70 Bq/sample) in an electrolyte solution. The main objective was to  
199 determine the ratio between the electrodeposited iron and the original iron content in the  
200 electrolyte solution. It was determined by measuring the mass difference of the stainless steel  
201 (SS) discs before and after the electrodeposition. This mass difference represented the yield of  
202 the electrodeposition process.

203 The addition of the <sup>55</sup>Fe standard solution was intended to investigate whether the gamma  
204 spectrometry results correspond to the yield of electrodeposited iron. The mass of the added <sup>55</sup>Fe  
205 standard solution was negligible; it therefore had no influence on the mass of the iron deposited  
206 on the SS discs or on the results of the ED yield.

207 In these experiments, the electrodeposition time (60, 90, and 180 minutes) and the amount of  
208 iron carrier (10 mg to 50 mg) were varied, while the current density of 0.190 A/cm<sup>2</sup> remained  
209 constant. In this way, the relationship between the ratio of electrodeposited iron and the original  
210 iron content and the time of ED was investigated. To stop the electrodeposition process, 1 ml of  
211 concentrated ammonium hydroxide was added to the electrochemical cell at the end of each  
212 experiment. The electrolyte solution was then removed from the cell, and the SS disc was  
213 washed with distilled water and ethanol, dried, and weighed. The thickness of the  
214 electrodeposited film for prepared samples was then calculated. For this purpose, the surface area

215 of the electrode, the yield of the electrodeposited film and the density value for  $\text{Fe}(\text{OH})_3$ , i.e.  
216  $4.25 \text{ g/cm}^2$  were taken into account. The literature indicates that iron in the form of  $\text{Fe}(\text{OH})_3$   
217 predominates in the deposited films, as the cathodic reduction increases the local pH near the  
218 electrode and leads to the deposition of metal hydroxides [38 - 42]. The activity of  $^{55}\text{Fe}$  was then  
219 determined by gamma spectrometry. The efficiency was determined by measuring the activity of  
220 these test solutions prepared by ED on the SS disc which showed direct correlation between the  
221 film thickness and the gamma spectrometry results. This was done for the additional check of  
222 determination of the activity of  $^{55}\text{Fe}$  in the samples by gamma spectrometry. The ED of iron was  
223 performed with two samples containing only 0.25 mg and 0.5 mg of iron, respectively, together  
224 with a  $^{55}\text{Fe}$  standard solution (70 Bq/sample) in electrolyte solution. That way, the sample  
225 thickness could be neglected, so that no effects on the gamma detection efficiency were to be  
226 expected.

227

#### 228 *Electrodeposition of iron from real concrete samples*

229 Based on the results obtained with the test solutions the optimum conditions for the  
230 electrodeposition of iron from real concrete samples were determined. The duration of the  
231 electrodeposition was set at 90 minutes at a current density of  $0.190 \text{ A/cm}^2$ . Concrete samples  
232 containing only iron, after undergoing the fusion process and separation of iron using TRU resin,  
233 were evaporated to dryness. The residue was then dissolved in an electrolyte solution and  
234 transferred to the electrochemical cell. After deposition, the SS cathode with the thin deposited  
235 iron film was washed with distilled water and ethanol, dried in air and the activity of  $^{55}\text{Fe}$  was  
236 determined by gamma spectrometry.

237 To further validate the method and confirm its applicability to real concrete samples and to  
238 ensure that the determined  $^{55}\text{Fe}$  activity is accurate, the standard addition method was applied.  
239 Hence, three concrete samples with unknown activities of  $^{55}\text{Fe}$  were taken and two aliquots  
240 (Aliquot 1 and Aliquot 2) were prepared from each sample. Aliquot 1 contained the pure sample,  
241 while Aliquot 2 was spiked with an additional known activity of a  $^{55}\text{Fe}$  standard solution (about  
242 2 Bq/g). For the method to be considered accurate, the measured activity of Aliquot 2 should be  
243 equal to the sum of the activity of Aliquot 1 and the added  $^{55}\text{Fe}$  standard solution activity  
244 (approximately 2 Bq/g). This relationship can be expressed as:

$$245 \quad A(\text{aliquot 2}) = A(\text{aliquot 1}) + A(^{55}\text{Fe})_{\text{added}} \quad (1)$$

246

#### 247 **Gamma ray spectrometric measurements**

248 Samples prepared as thin films were placed in the plastic foil to prevent contamination.  
249 For counting, the samples were placed directly above the carbon-epoxy opening window of the  
250 high purity germanium (HPGe) detector, minimizing low energy gamma ray attenuation and  
251 maximizing efficiency. Measurements were conducted using a Canberra's broad energy planar  
252 HPGe detector with relative efficiency of 48%, a carbon epoxy window and an energy range of 4  
253 to 2000 keV placed in the lead shielding. The DSA-LX Digital Signal Analyser electronic was  
254 used with Genie 2000 software for data acquisition and analyses. The spectrum collection times  
255 for the prepared samples ranged from 10 000 seconds to 200 000 seconds, depending on the  
256 activity, to reach similar counting statistics and comparable measurement uncertainties, when  
257 possible. Background measurements lasting 300 000 seconds were performed and subtracted  
258 from the sample spectra. The combined uncertainty budget of the activity measurement included  
259 the highest contributors, namely the uncertainty of determining the net area of the photo peak

260 and the efficiency uncertainty. Efficiency calibration was performed mathematically using the  
261 LabSOCS tool and extrapolation to the energy of interest. These calibrations were then checked,  
262 corrected and optimized using a  $^{55}\text{Fe}$  point source of known activity. Additionally, samples  
263 prepared by electrodeposition on SS plate and on filters using APDC method, combined with a  
264  $^{55}\text{Fe}$  standard solution of known activity, were measured to confirm calibration. The obtained  
265 efficiency was used as a starting point for determining the activities in further test measurements  
266 and analysing attenuation as a function of total amount of iron in the sample. The corrections of  
267 the efficiency were obtained experimentally by preparing and measuring the samples by varying  
268 the initial amount of iron.

## 269 **Results**

### 270 **APDC precipitation of iron from real concrete samples**

271 The results of the measured ( $A_{\text{measured}}$ ) versus target ( $A_{\text{target}}$ ) activities for  $^{55}\text{Fe}$  in five concrete  
272 samples with different total iron contents are shown in Table 1. The iron content in these samples  
273 ranged from 0.05 mg to 1.00 mg. The comparison between the activities measured by gamma  
274 spectrometry and the target values shows that the discrepancy of gamma measurements is less  
275 than 17% for samples with a total iron content of less than 0.45 mg. However, when the iron  
276 content increases above this threshold, the discrepancy increases and reaches up to 53% for  
277 samples with 1.0 mg of iron.

278 Table 1 also shows the results of measured activities ( $A_{\text{measured}}$ ) for  $^{55}\text{Fe}$  obtained with two  
279 different detectors in two different facilities for all five samples. The comparison shows that the  
280 largest difference in  $^{55}\text{Fe}$  activity between the measurements of IRB and IJS is 9% for the  
281 Concrete -2- sample. The maximum difference for other samples is 3%. The excellent agreement  
282 of the results between two laboratories, which are within the uncertainties, indicates that the

283 discrepancy between the measured and targeted activity values comes from sample preparation,  
284 and is not measurement related.

285

**Table 1** Dependence of measured  $^{55}\text{Fe}$  activity (measured by gamma ray spectrometry) on total iron mass in concrete samples prepared by APDC precipitation: a comparative study between two different laboratories

Sample	$m(\text{Fe})_{\text{total}}/\text{mg}$	$A_{\text{target}}/\text{Bq}$	IRB	IJS
			$A_{\text{meas.}}/\text{Bq}$	$A_{\text{meas.}}/\text{Bq}$
Concrete -1-	0.05	5	$4.9 \pm 0.5$	$4.9 \pm 0.6$
Concrete -2-	0.30	10	$8.7 \pm 0.9$	$9.6 \pm 0.8$
Concrete -3-	0.45	15	$12.4 \pm 1.4$	$12.7 \pm 1.1$
Concrete -4-	0.90	30	$18.5 \pm 2.0$	$19.5 \pm 1.3$
Concrete -5-	1.00	35	$17.6 \pm 1.9$	$16.4 \pm 3.0$

286

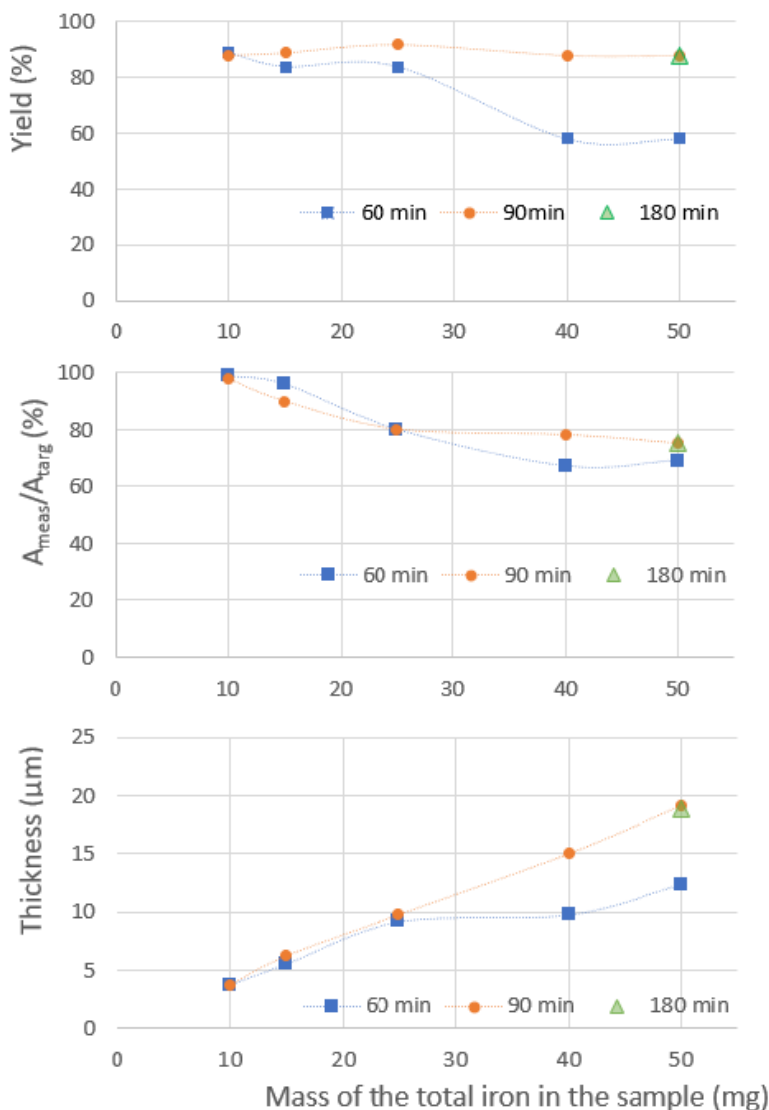
287

## 288 **Electrodeposition**

289 Fig. 2 shows the results of the ED for the test samples and illustrates the relationship  
290 between the time of the ED, the yield of the ED and the total iron content in the electrolyte  
291 solution. In order to better follow the obtained results, the measurement data shown by marks in  
292 Fig. 2 are linked by the dashed curves, which however do not present interpolation of yield,  
293 activities or samples masses.

294 The results can be categorized into three different groups: group one, in which the ED  
295 yield remains the same regardless of whether the ED time is 60 or 90 minutes. This applies to  
296 samples containing 10 mg and 15 mg total iron. Group two, in which the sample contains 25 mg  
297 of total iron. Here, an extension of the ED time to 90 minutes leads to an up to 8 % higher yield  
298 compared to a 60 minutes ED time. Group three, in which the ED yield increases by 30 % when  
299 the ED time is extended to 90 minutes. To investigate the effects of further increasing the ED

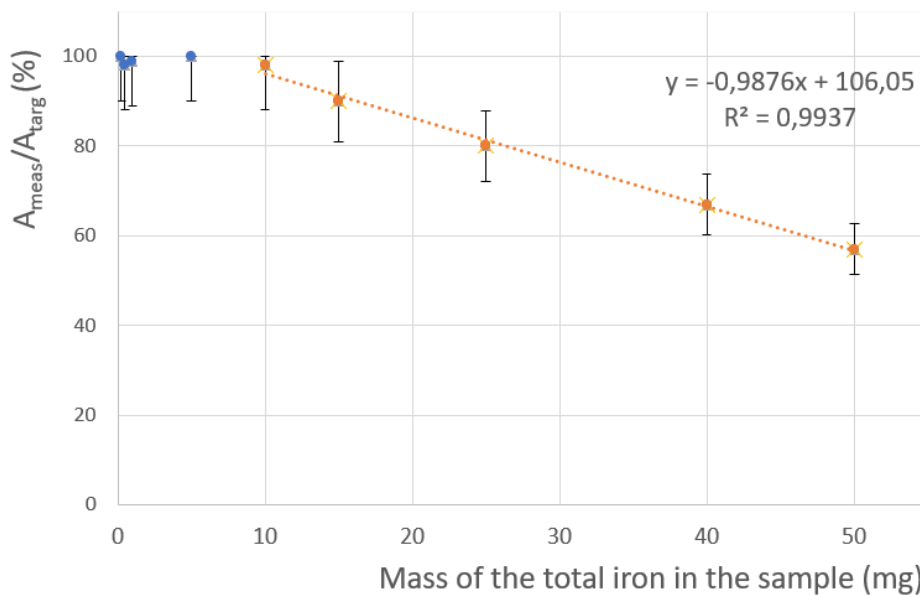
300 time, a few experiments were conducted where the ED time was 180 minutes. However, this  
 301 further increase in ED time did not lead to an additional improvement in yield.



302  
 303 Fig. 2 Electrodeposition yield, measured activity values regarding the targeted ones and film  
 304 thickness for test solutions with varying total iron content and electrodeposition times

305  
 306 A similar trend can be observed in the gamma spectrometry results, which are also shown in  
 307 Fig. 2. As the total iron content increases, the discrepancies in the results become more  
 308 pronounced, reaching up to 25 % for samples with an original iron content of 50 mg. For these

309 high-iron samples, a correction factor should be introduced, even after the yield corrected results.  
310 Fig. 3 illustrates the required correction of the efficiency (%) as a function of the total iron  
311 content and shows a linear dependence within the analysed range of 10 – 50 mg.  
312 The same observation can be made when considering the relationship between the thickness of  
313 electrodeposited film, influencing directly the detection efficiency, and the discrepancy in the  
314 results obtained by gamma spectrometry (Fig. 2).  
315 In addition to the results shown in Fig. 2, the activity of  $^{55}\text{Fe}$  was determined by gamma  
316 spectrometry in two further samples with 0.25 mg and 0.50 mg total iron. For these samples, the  
317 gamma spectrometric measurements showed excellent agreement with the target value with  
318 maximum discrepancies of only 5 %.  
319



320  
321 **Fig. 3** Correlation between the total iron content in the sample (mg) and the correction of the  
322 detection efficiency

323

324 The results obtained with the standard addition method, used for real concrete samples, show  
325 excellent consistency between mutual aliquots of all three samples. The deviation of activities  
326 between two aliquots of the same sample was not more than 10 %.

327

## 328 **Discussion**

329 Iron precipitation using APDC has previously been used alongside gamma spectrometry,  
330 with known problems such as lack of selectivity in iron complex formation and attenuation. The  
331 aim of this study was to determine the maximum amount of total iron in real concrete samples at  
332 which the exact activity of  $^{55}\text{Fe}$ , prepared with APDC and measured by gamma spectrometry,  
333 can still be accurately determined. The results for five concrete samples containing different  
334 amounts of total iron are shown in Table 1. As expected, the discrepancy in the gamma  
335 measurements increased with higher total iron content, which directly shows the influence of  
336 attenuation. The significant increase in discrepancy can already be seen for samples with less  
337 than 1.0 mg of total iron, leading to the conclusion that this method can only be considered  
338 reliable for samples with a total iron content of 0.50 mg or less. Along with the thickness, the  
339 nonpredictable possible inhomogeneity of samples prepared in this way could still result in  
340 doubtful results.

341 On the other hand, for the ED preparation method, the effects of the different amounts of total  
342 iron in the analyzed samples on the ED yield and the measured activity values of  $^{55}\text{Fe}$  were  
343 investigated. The duration of the ED was optimized to maximize the yield. The results indicate  
344 that under the specified conditions, such as the size of the electrochemical cell, the diameter of  
345 the cathode, and the volume of electrolyte, the optimal ED duration is 90 minutes. While a  
346 shorter duration of 60 minutes is sufficient to achieve maximum yield in samples with lower

347 total iron content (up to 25 mg), for actual concrete samples with unknown total iron content, 90  
348 minutes is necessary to ensure maximum ED yield, regardless of the total iron mass. These  
349 optimized ED conditions were applied to real concrete samples to confirm the method's  
350 applicability. The standard addition method was used, and the results from Aliquots 1 and 2 of  
351 the same sample were consistent, with discrepancies under 10%.

352 When analyzing the gamma spectrometry results, a clear correlation emerged between the total  
353 iron mass and the discrepancy between the measured and target activity values (Fig. 2) as a result  
354 of attenuation. Introduction of correction for the efficiency as a function of total iron content is  
355 thus necessary. The obtained correlation is presented in Fig. 3.

356

357

## 358 **Conclusion**

359 This study emphasizes the potential of gamma spectrometry as the method for the determination  
360 of  $^{55}\text{Fe}$  in complex solid samples with high amount of iron such as concrete and metals from  
361 NPP radioactive waste. A key challenge of this method is the low energy of the emitted ray,  
362 which causes significant attenuation. Therefore, the preparation of a thin and homogenous  
363 sample is crucial.

364 In the study, two sample preparation techniques for gamma measurements were compared:  
365 APDC precipitation method and electrodeposition. The APDC precipitation method has  
366 limitations in accuracy for samples with higher iron content though it remains reliable for  
367 samples with less than 0.50 mg total iron. On the other hand, the ED proved to be reliable for  
368 samples containing up to 50 mg of iron. The duration of the ED was optimized to 90 minutes to  
369 achieve the maximum yield.

370 For the activity measurements, an experimental correlation function for the detection  
371 performance of the gamma spectrometry system was introduced as a function of the total iron  
372 content. This function can be used in future measurements.

373 It is expected that further optimization of the electrochemical cell will increase efficiencies and  
374 lower detection limits. These improvements are of utmost importance for the fast and accurate  
375 determination of  $^{55}\text{Fe}$  activity and activities of other radionuclides in samples from NPPs and  
376 accelerators, where precise analysis is essential after decomposition.

377

### 378 **Acknowledgements**

379 This work was supported by the Ministry of Science and Education of the Republic of Croatia,  
380 Croatian-Slovenian bilateral scientific project: *Gamma spectrometric determination of low level*  
381 *activity of low-energetic radionuclides in complex samples.*

### 382 **Declarations**

#### 383 **Conflict of interest**

384 The authors declare that they have no conflict of interest.

#### 385 **Data availability**

386 The data generated and analyzed in this study are available from the corresponding author upon  
387 request.

388

389 **Author contributions statement**

390 All authors contributed to this article. Conceptualization: Katja Magdić Košiček, Ivana  
391 Tucaković, Benjamin Zorko; Methodology: Ljudmila Benedik, Marijan Nečemer, Katja Magdić  
392 Košiček, Ivana Tucaković; Formal analysis and investigation: Benjamin Zorko, Marijan  
393 Nečemer, Branko Vodenik, Ljudmila Benedik, Ivana Tucaković; Writing - original draft  
394 preparation: Katja Magdić Košiček, Ivana Tucaković; Writing - review and editing: Ljudmila  
395 Benedik, Benjamin Zorko, Marijan Nečemer, Branko Vodenik, Željko Grahek; Supervision:  
396 Željko Grahek, Benjamin Zorko;

397

398

399 **References:**

- 400 1. World nuclear association [WWW Document], 2021. URL [https://www.world-](https://www.world-nuclear.org/information-library/current-and-future-generation/nuclear-power-in-the-world-today.aspx)  
401 [nuclear.org/information-library/current-and-future-generation/nuclear-power-in-the-](https://www.world-nuclear.org/information-library/current-and-future-generation/nuclear-power-in-the-world-today.aspx)  
402 [world-today.aspx](https://www.world-nuclear.org/information-library/current-and-future-generation/nuclear-power-in-the-world-today.aspx) (accessed 3.23.21).
- 403 2. IURCHAK, D., 2021. 200 - 400 Nuclear Reactors to be Decommissioned by 2040 1–8.
- 404 3. Decommissioning [WWW Document], n.d. URL  
405 <https://www.iaea.org/topics/decommissioning>
- 406 4. IAEA Nuclear Energy Series No. NW-T-1.24 [WWW Document], 2013. URL  
407 [https://www-pub.iaea.org/MTCD/Publications/PDF/Pub1601\\_web.pdf](https://www-pub.iaea.org/MTCD/Publications/PDF/Pub1601_web.pdf)
- 408 5. Stanford University, n.d. Fe-55 radionuclide fact sheet [WWW Document]. URL  
409 <https://ehs.stanford.edu/reference/fe-55-radionuclide-fact-sheet>
- 410 6. Curioni, A., Dinar, N., La Torre, F.P., Leidner, J., Murtas, F., Puddu, S., Silari, M., 2017.  
411 Measurements of <sup>55</sup>Fe activity in activated steel samples with GEMPix. Nucl.  
412 Instruments Methods Phys. Res. Sect. A Accel. Spectrometers, Detect. Assoc. Equip.  
413 849, 60–71. <https://doi.org/10.1016/j.nima.2016.12.059>
- 414 7. IAEA, 2009. Determination and use of scaling factors for waste characterization in  
415 nuclear power plants. p. NW-T-1.18.
- 416 8. IAEA, 2007. Strategy and Methodology for Radioactive Waste Characterization.
- 417 9. Lee, Y.J., Lim, J.M., Lee, J.H., Hong, S.B., Kim, H., 2020. Analytical method for  
418 determination of <sup>41</sup>Ca in radioactive concrete. Nucl. Eng. Technol.  
419 <https://doi.org/10.1016/j.net.2020.09.020>
- 420 10. Gautier, C., Laporte, E., Lambrot, G., Giuliani, M., Colin, C., Bubendorff, J., Crozet, M.,  
421 Mougél, C., 2020. Accurate measurement of <sup>55</sup>Fe in radioactive waste. J. Radioanal.  
422 Nucl. Chem. 326, 591–601. <https://doi.org/10.1007/s10967-020-07332-0>

- 423 11. Grahek, Ž., Mačefat, M.R., 2004. Isolation of iron and strontium from liquid samples and  
424 determination of  $^{55}\text{Fe}$  and  $^{89,90}\text{Sr}$  in liquid radioactive waste. *Anal. Chim. Acta* 511,  
425 339–348. <https://doi.org/10.1016/j.aca.2004.01.049>
- 426 12. Warwick, P.E., Croudace, I.W., 2006. Isolation and quantification of  $^{55}\text{Fe}$  and  $^{63}\text{Ni}$  in  
427 reactor effluents using extraction chromatography and liquid scintillation analysis. *Anal.*  
428 *Chim. Acta* 567, 277–285. <https://doi.org/10.1016/j.aca.2006.03.043>
- 429 13. Chu, C.M., 2003. The effect of complexing agents on the electrodeposition of Fe-Ni  
430 powders. *J. Chinese Inst. Chem. Eng.* 34, 689–695.
- 431 14. Chu, C.M., Wan, C.C., 1992. The effect of chelating agents on the cathodic polarization  
432 and the electrodeposition of iron powders. *J. Mater. Sci.* 27, 6700–6706.  
433 <https://doi.org/10.1007/BF01165957>
- 434 15. Deelo, M., Weil, K., Osseop-Asare, K., 2006. Electrodeposition of Iron in Aqueous  
435 Ferrous Sulfate Solution: Role of Ammonium Ion 2, 293–302.
- 436 16. Díaz, S.L., Calderón, J.A., Barcia, O.E., Mattos, O.R., 2008. Electrodeposition of iron in  
437 sulphate solutions. *Electrochim. Acta* 53, 7426–7435.  
438 <https://doi.org/10.1016/j.electacta.2008.01.015>
- 439 17. Evreinova, N. V., Shoshina, I.A., Naraev, V.N., Tikhonov, K.I., 2008. Electrodeposition  
440 of iron from sulfate solutions in the presence of aminoacetic acid. *Russ. J. Appl. Chem.*  
441 81, 1180–1183. <https://doi.org/10.1134/S1070427208070100>
- 442 18. Zhang, Z., Kitada, A., Fukami, K., Yao, Z., Murase, K., 2020. Electrodeposition of an  
443 iron thin film with compact and smooth morphology using an ethereal electrolyte,  
444 *Electrochimica Acta*, 348, 136289, <https://doi.org/10.1016/j.electacta.2020.136289> 0013-  
445 4686/
- 446 19. Meng, Q., Wang, Z., Chai, X., Weng, Z., Ding, R., Dong, L., 2016. Fabrication of  
447 Hematite ( $\alpha\text{-Fe}_2\text{O}_3$ ) Nanoparticles Using Electrochemical Deposition, *Applied Surface*  
448 *Science*, 368, 303 -308 <http://dx.doi.org/10.1016/j.apsusc.2016.02.007>
- 449 20. Yanga, Q., Lana, C., Wangc, Y., Zhaoa, Z., Lia, B., 2020. Recycling of ultrafine NdFeB  
450 waste by the selective precipitation of rare earth and the electrodeposition of iron in  
451 hydrofluoric acid, *Separation and Purification Technology*, 230, 115870,  
452 <https://doi.org/10.1016/j.seppur.2019.115870>
- 453 21. Kumar, M., Gandhi, S.S., Udhayakumar, J., Satpati, A., Shukla, R., Tyagi, A.K., Dash,  
454 A., 2013. An electrochemical technique to prepare  $^{55}\text{Fe}$  source for the calibration of the  
455 X-ray detectors. *Radiochim. Acta* 101, 185–193. <https://doi.org/10.1524/ract.2013.2012>
- 456 22. Labeyrie, L. D., Livingston, H. D., Gordon, A.G., 1975. Measurement of  $^{55}\text{Fe}$  from  
457 nuclear fallout in marine sediments and seawater. *Nucl. instruments m* 128, 575–580.
- 458 23. Skwarzec, B., Holm, E., Struminska, D.I., 2001. Radioanalytical determination of Fe-55  
459 and Ni-63 in the environmental samples. *Chem. Analityczna* 46, 23–30.
- 460 24. Skwarzec, B., Strumińska, D.I., 2006. Radionuclides of iron (  $^{55}\text{Fe}$  ), nickel (  $^{63}\text{Ni}$  ),  
461 polonium (  $^{210}\text{Po}$  ), uranium (  $^{234}\text{U}$  ,  $^{235}\text{U}$  ,  $^{238}\text{U}$  ) and plutonium (  $^{238}\text{Pu}$  ,  $^{239}$  +  
462  $^{240}\text{Pu}$  ,  $^{241}\text{Pu}$  ) in Poland and Baltic Sea environment 51.

- 463 25. Kane, S., Lazo, P., Ylli, F., Stafilov, T., Qarri, F., Marku, E., 2016. Separation of heavy  
464 metal from water samples—The study of the synthesis of complex compounds of heavy  
465 metal with dithiocarbamates. *J. Environ. Sci. Health Part A*, 51, 335–340.
- 466 26. Nabipour, H., Ghammamy, S., Ashuri, S., Aghbolaghc, Z.S., 2010. Synthesis of a new  
467 dithiocarbamate compound and Study of Its biological properties. *J. Org. Chem.*, 2, 75–  
468 80;
- 469 27. Abu-El-Halawa, R., Zabin, S.A., 2017. Removal efficiency of Pb, Cd, Cu and Zn from  
470 polluted water using dithiocarbamate ligands. *J. Taibah Univ. Sci.* 2017, 11, 57–65.
- 471 28. Ajiboye, T. O., Ajiboye, T. T., Marzouki, R., Onwudiwe, D. C., 2022. The Versatility in  
472 the Applications of Dithiocarbamates, 23, 1317, *International Journal of Molecular*  
473 *Science*
- 474 29. Nečemer, M., Kump, P., 1999. Application of ammonium pyrrolidinedithiocarbamate  
475 precipitation and X-ray spectrometry in the analysis of <sup>55</sup>Fe in nuclear liquid wastes.  
476 *Spectrochim. acta, Part B At. Spectrosc.* 54, 621–625. [https://doi.org/10.1016/S0584-](https://doi.org/10.1016/S0584-8547(99)00018-X)  
477 [8547\(99\)00018-X](https://doi.org/10.1016/S0584-8547(99)00018-X)
- 478 30. Giokas, D. L., Paleologos, E. K., Karayannis, M. I., 2002. Speciation of Fe(II) and Fe(III)  
479 by the modified ferrozine method, FIA-spectrophotometry, and flame AAS after cloud-  
480 point extraction, *Anal. Bioanal. Chem.*, 373, 4 – 5, doi: 10.1007/s00216-002-1326-7
- 481 31. Trdin, M., Benedik, L., 2017. Fast Decomposition Procedure of Solid Samples by  
482 Lithium Borates Fusion Employing Salicylic Acid.  
483 <https://doi.org/10.1021/acs.analchem.6b04980>
- 484 32. Oh, J.S., Warwick, P. E., Croudace, I. W., Lee, S. H., 2014. Evaluation of three  
485 electrodeposition procedures for uranium, plutonium and americium. *Applied Radiation*  
486 *Isotopes*, 87, 233 – 237, <https://doi.org/10.1016/j.apradiso.2013.11.048>;
- 487 33. Jia, G., Torri, G., Innocenzi, P., Di Lullo, A., 2005. Determination of radium isotopes in  
488 mineral water 12 samples by  $\alpha$ -spectrometry. *International Congress Series*, 1276, 412 –  
489 414 doi:10.1016/j.ics.2004.09.019;
- 490 34. Krmpotić M., Rožmarić M., Benedik Lj., 2018. Investigation of key factors in  
491 preparation of alpha sources by electrodeposition. *Applied Radiation and Isotopes*, 136,  
492 37 – 44
- 493 35. Puphal, K.W., Olsen, D.R., 1972. Electrodeposition of alpha-emitting nuclides from a  
494 mixed oxalate-chloride electrolyte. *Anal. Chem.* 44, 284–289.
- 495 36. B. E. Conway, *Electrochemical supercapacitors, Scientific Fundamentals and*  
496 *Technological Applications*, Chapter 13, pg: 337 – 340.
- 497 37. Mahapatro, A., Kumar Suggu, S., 2018., Modeling and simulation of electrodeposition:  
498 Effect of electrolyte current density and conductivity on electroplating thickness,  
499 *Advanced Materials Science*, 3 (2), 1 – 9, doi: 10.15761/AMS.1000143
- 500 38. Yan, Z., Sun, H., Chen, X., Liu, H., Zhao, Y., Li, H., Xie, W., Cheng, F., Chen, J., 2018.  
501 Anion insertion enhanced electrodeposition of robust metal hydroxide/oxide electrodes  
502 for oxygen evolution, *Nature communication*, 9, 2372, doi: 10.1038/s41467-018-04788-3

- 503 39. Le Manh, T., Arce-Estrada, E.M., Caballero, M., Clemente, R., Sanceh, W., Gonzalez, J.  
504 A., Rojas, L., Romo, R., Pardave, M.P., 2018. Iron Electrodeposition from Fe(II) Ions  
505 Dissolved In A Choline Chloride: Urea Eutectic Mixture, 165, 16, D1 – D5, doi:  
506 10.1149/2.0561816jes
- 507 40. Hansen, P. G., 1959. The conditions for electrodeposition of insoluble hydroxides at a  
508 cathode surface: a theoretical investigation, *Journal of Inorganic and Nuclear Chemistry*,  
509 12, 30 – 37
- 510 41. Hansen, P. G., 1961. The electrodeposition of insoluble hydroxides – an experimental  
511 investigation, *Journal of Inorganic and Nuclear Chemistry*, 17, 232 – 239,
- 512 42. Beesley, A. M., Crespo, M. T., Weiher, N., Tsapatsaris, N., Cózar, J.S., Esparza, H.,  
513 Méndez, C. G., Hill, P., Schroeder S. L. M., Montero-Cabrera, M. E., 2009 Evolution of  
514 chemical species during electrodeposition of uranium for alpha spectrometry by the  
515 Hallstadius method, *Applied Radiation and Isotopes*, 67, 1559 - 1569